OXFORD

Cerebral Cortex, 2023, **33**, 2901–2911
https://doi.org/10.1093/cercor/bhac248
Advance access publication date 31 July 2022
Original Article

The characteristics of glucose metabolism and functional connectivity in posterior default network during nondemented aging: relationship with executive function performance

Kai Xu[1,2,†], Na Niu[3,†], Xin Li[2,4,†], Yuan Chen[2,4], Dandan Wang[2,4], Junying Zhang[4,5], Yaojing Chen[2,4], He Li[4,5], Dongfeng Wei[4,5], Kewei Chen[4,6], Ruixue Cui[3,*], Zhanjun Zhang[2,4,*], Li Yao[1,*]

[1]School of Artificial Intelligence, Beijing Normal University, Beijing 100875, P.R. China,
[2]State Key Laboratory of Cognitive Neuroscience and Learning, Beijing Normal University, Beijing 100875, P.R. China,
[3]Department of Nuclear Medicine, Peking Union Medical College Hospital, Peking Union Medical College, Chinese Academy of Medical Sciences, No1 Shuaifuyuan,Wangfujing St., Dongcheng District, Beijing 100730, P.R. China,
[4]BABRI Centre, Beijing Normal University, Beijing 100875, P.R. China,
[5]Institute of Basic Research in Clinical Medicine, China Academy of Traditional Chinese Medicine, Beijing 10070, P.R. China,
[6]Department of Neurology, University of Arizona College of Medicine, Phoenix, AZ 85006, United States
*Corresponding authors: No. 19, XinJieKouWai St., HaiDian District, Beijing 100875, China. Tel./Fax: +86 1058803882; E-mail: yaoli@bnu.edu.cn (Li Yao); No.1 Shuaifuyuan Wangfujing Dongcheng District, Beijing 100730, China. Tel./Fax: +86 1069156114; E-mail: mmdhmm@126.com (Ruixue Cui); No. 19, XinJieKouWai St., HaiDian District, Beijing 100875, China. Tel./Fax: +86 1058802005; E-mail: zhang_rzs@bnu.edu.cn (Zhanjun Zhang)
†Kai Xu, Na Niu, and Xin Li are co-first authors contributed to the work equally.

Background: Understanding the characteristics of intrinsic connectivity networks (ICNs) in terms of both glucose metabolism and functional connectivity (FC) is important for revealing cognitive aging and neurodegeneration, but the relationships between these two aspects during aging has not been well established in older adults.
Objective: This study is to assess the relationship between age-related glucose metabolism and FC in key ICNs, and their direct or indirect effects on cognitive deficits in older adults.
Methods: We estimated the individual-level standard uptake value ratio (SUVr) and FC of eleven ICNs in 59 cognitively unimpaired older adults, then analyzed the associations of SUVr and FC of each ICN and their relationships with cognitive performance.
Results: The results showed both the SUVr and FC in the posterior default mode network (pDMN) had a significant decline with age, and the association between them was also significant. Moreover, both decline of metabolism and FC in the pDMN were significantly correlated with executive function decline. Finally, mediation analysis revealed the glucose metabolism mediated the FC decline with age and FC mediated the executive function deficits.
Conclusions: Our findings indicated that covariance between glucose metabolism and FC in the pDMN is one of the main routes that contributes to age-related executive function decline.

Key words: brain aging; executive function; functional connectivity; glucose metabolism; posterior default mode network.

Introduction

Aging is accompanied by brain function decline as well as neuronal degeneration. Using fluorine-18-fluorodeoxyglucose positron emission tomography (^{18}F-FDG PET), studies in normal healthy individuals have consistently shown decreased cerebral glucose metabolism with increasing age, with differential effects across brain regions (Kalpouzos et al. 2009; Hsieh et al. 2012). The regions that are most affected by aging form a spatial pattern including the cingulate gyrus and frontal areas (Chetelat et al. 2013). Such a spatial pattern is potentially a sensitive biomarker for discriminating normal aging from Alzheimer's disease, as well as from other neurodegenerative diseases (Mosconi 2005). On the other hand, recent resting-state functional magnetic resonance imaging (fMRI) researches have provided ample evidence that aging and neurodegeneration are also related to the breakdown of functional networks. Age-related functional connectivity (FC) disruptions have been specifically reported in multiple intrinsic connectivity networks (ICNs) in the brain (Laird et al. 2011; Ferreira and Busatto 2013). These ICNs typically integrate information across a wide range of tasks and across multiple brain functions (Damoiseaux et al. 2008; Zhang et al. 2014). Thus, to further understand the processes underlying age-related brain changes, alterations in the FC in some key brain networks should also be explored in combination with cerebral metabolism decline in the context of age variation (Ferreira and Busatto 2013).

Received: March 28, 2022. **Revised:** May 20, 2022. **Accepted:** May 21, 2022

Understanding the neuroimaging characteristics of ICNs in terms of both glucose metabolism and FC is important for revealing brain aging. A mechanistic view linking FC to the hypometabolism, however, has been lacking so far. A few multimodal imaging studies using FDG-PET and resting-state fMRI approached the question of whether local FC of ICNs is correlated with their local levels of glucose metabolism. These studies showed that the correlation was discordant in different networks and changed with aging as well as disease stages. Among previous studies, there seems to be a stable result that the posterior default mode network (pDMN) (include cingulate gyrus and precuneus [PCu]) areas unite the 2 dimensions signally. Firstly, the pDMN are the hub regions for brain information communication and neural integration (van den Heuvel et al. 2013). Frequent and massive information operations require high energy consumption. Other the other hand, areas of this network show the highest level of glucose use among the whole cerebral cortex in humans (Gusnard and Raichle 2001). The phenomenon that pDMN had the highest extent of both concurrent energy utilization and neuronal activity (Shokri-Kojori et al. 2019), rendered these hub regions more vulnerable to neurodegenerative conditions such as Alzheimer's disease (Tomasi et al. 2013). Some other previous studies (Arenaza-Urquijo et al. 2013; Chetelat et al. 2013; Wagner et al. 2016; Verger et al. 2017) have indicated that local metabolic dysfunction may be due to or may lead to disruption in FC with distant brain regions. It is likely that glucose metabolism disturbance may impact myelin integrity or other components that lead to dysfunction in connected brain regions (Bartzokis 2004). Measures of FC and glucose metabolism are usually not characterized as processes, but they may reflect relevant physiological processes, assessing the relationship between them is a stepping-stone to a better understanding of the physiological mechanisms underlying age-related metabolic decline and neurodegeneration.

However, the relationships between aging, energy metabolism, functional-level network properties and cognitive performances have not been widely and systematically evaluated (Chetelat et al. 2013). One recent study assessed the relationship between age-related metabolism decrease and networks segregation changes in sensorimotor networks (Manza et al. 2020), but there was little study so far that explored the interaction effects of aging on glucose energy metabolism and network FC changes in DMN, which were mentioned above having closer relationships to cognitive aging and neurodegenerative diseases (Buckner and Krienen 2013; Douaud et al. 2014), and their contribution to cognitive decline in older individuals. The objective of the present study was to assess the relationship between age-related glucose metabolism and FC in key ICNs like pDMN, and the direct or indirect effects on cognitive deficits in older adults.

Materials and methods

Participants

All participants enrolled in this study were from the Beijing Aging Brain Rejuvenation Initiative (BABRI), which is an ongoing community-based cohort study in China focusing on dementia prevention and early detection of cognitive impairment (Yang et al. 2021). Participants were urban nondemented older individuals living in local communities in Beijing and were all right-handed native Chinese speakers. The inclusion criteria were (i) being at least 55 years old; (ii) no dementia or probable dementia according to the DSM-IV-TR (American Psychiatric Association 2000); (iii) no history of neurological, psychiatric, or systemic illnesses known to influence cerebral function, including serious vascular diseases, head trauma, tumor, current depression, alcoholism, and epilepsy; and (iv) no prior history of taking psychoactive medications. The experiments were undertaken with the understanding and written consent of each subject and with the Ethics Committee and Institutional Review Board of Beijing Normal University's approval (ICBIR_A_0041_002.02). During the time of this investigation, we identified 59 BABRI participants (31 males and 28 females) whose ^{18}F-FDG PET and resting-state fMRI data were available for the purpose of our study. The interval between ^{18}F-FDG PET data and MRI data acquisition was no more than 3 months, with an average interval of <1 month.

Neuropsychological testing

All 59 participants received a widely used screening test for general cognitive ability and several classic neuropsychological tests, including the Mini-Mental State Examination (MMSE), and some tests that assess specific cognitive functions in aging research: (i) the Auditory Verbal Learning Test (AVLT), (ii) Boston Naming Test (BNT), (iii) Clock-Drawing Test (CDT), (iv) Category Verbal Fluency Test (CVFT), (v) Digit Span, (vi) Rey–Osterrieth Complex Figure (ROCF) delayed recall and copy test, (vii) Symbol Digit Modifying Test (SDMT), (viii) Stroop Color and Word Test, and (ix) Trail Making Test (TMT). The specific neuropsychological test procedures have been described in our previous work (Wang et al. 2013; Lu et al. 2020). The neuropsychological tests of each participant were operated in their living communities by experienced graduate students no more than 1 week before or after he or she was invited for the MRI scan.

Imaging data acquisition and preprocessing

All participants underwent an ^{18}F-FDG PET scan using a Biograph 64 TruePoint TrueV PET/CT system (Siemens Medical Solutions, Germany) at Peking Union Medical College Hospital, Peking Union Medical College (Beijing, China). All participants started the PET scan 40–60 minutes after the intravenous injection of 5.55 MBq/kg (0.15 mCi/kg) ^{18}F-FDG produced using an RDS-111

Cyclotron (CTI, US) after participants had fasted for at least 4 hours and their blood glucose level was ensured not to exceed the normal limit (6.4 mmol/L). All participants were required to close their eyes after tracer injection to eliminate an unwanted elevated uptake of FDG into the occipital lobe. The scan lasted 10 minutes. ^{18}F-FDG PET images were acquired with 148 axial slides with an interslice spacing of 3 mm, and the camera resolution is 4 mm (Yuan et al. 2016). PET images were visually read by 2 experienced nuclear medicine physicians.

For the MRI data, all participants were scanned on a 3.0 T Siemens scanner during a single session, wherein high-resolution T1-weighted structural MRIs and resting-state functional scans were obtained. Resting-state data were collected using an echo-planar imaging sequence that consisted of an echo time (TE) = 30 ms, repetition time (TR) = 2000 ms, flip angle = 90°, 33 axial slices, slice thickness = 3.5 mm, acquisition matrix = 64 × 64, and field of view (FOV) =200 × 200 mm^2. During the single-run resting acquisition, participants were instructed to stay awake, relax with their eyes closed, and remain as motionless as possible. Acquisition in the resting state lasted for 8 minutes, and 240 image volumes were obtained. T1-weighted, sagittal 3D magnetization prepared rapid gradient echo sequences that covered the entire brain (176 sagittal slices, TR = 1900 ms, TE = 3.44 ms, slice thickness = 1 mm, flip angle = 9°, inversion time = 900 ms, FOV = 256 × 256 mm^2, and acquisition matrix = 256 × 256) were also collected.

^{18}F-FDG PET data were preprocessed (Chen et al. 2009) with Statistical Parametric Mapping software (SPM12, http://www.fil.ion.ucl.ac.uk/spm). Briefly, automated segmentation and normalization procedures (Good et al. 2001) were applied to each subject's MRI to exclude non-brain tissue and to generate maps of smoothed gray matter density after spatial deformation into the Montreal Neurological Institute (MNI) template space. Automated algorithms were applied to each subject's PET image, coregistering to his/her T1 MRI and warped into the MNI template space using the normalization parameters derived from the MRI segmentation and normalization procedures. The PET images were then resampled to the same slice, matrix, and voxel size of the MNI template space, with a 91 × 109 × 91 data matrix and a voxel size of 2 × 2 × 2 mm^3. Finally, PET images were smoothed further with a 6-mm full width at half maximum (FWHM) Gaussian kernel. The standard uptake value ratio (SUVr) of each voxel was computed by normalizing each participant's ^{18}F-FDG PET data with the subject's mean FDG uptake value of cerebellar vermis (Barthel et al. 2015) (Anatomical Automatic Labeling (AAL) template regions number from 109 to 116 in the MNI template space).

The preprocessing of the resting-state fMRI data was carried out using SPM12 and Data Processing Assistant for Resting-State fMRI (Chao Gan and Yu Feng 2010). The steps of resting-state fMRI data preprocessing included the conversion of the Digital Imaging and Communications in Medicine (DICOM) data to Neuroimaging Informatics Technology Initiative (NIFTI) images; the removal of the first 10 time points from each patient's data; slice timing correction; realignment to the middle image; the regression of nuisance covariates, such as head motion, white matter signals, and cerebrospinal fluid (CSF) signals; spatial normalization by Diffeomorphic Anatomical Registration Through Exponentiated Lie Algebra (DARTEL); spatial smoothing with a 6-mm Full Width at Half Maxima (FWHM) Gaussian kernel; linear detrend and 0.01–0.08-Hz bandpass filtering.

Imaging data analysis

The main analysis procedure is shown in Supplementary Fig. 1. We performed independent component analysis (ICA) using the GIFT v4.0a software package (Calhoun et al. 2001) to decompose all of the resting-state data into 20 components following the practice described in a previous study (Jones et al. 2016). Principal components analysis is used as a technique to reduce the dimensions. Two data reduction steps are used for multisubject analysis. We used informax ICA algorithms as it maximizes the information transfer from the input to the output of a network. ICNs were identified with a template-matching procedure against a set of previously defined network maps (Greicius et al. 2004; Shirer et al. 2012). Spatial–temporal regression as a back-reconstruction method was used to acquire the individual-level FC strength of each network (Filippini et al. 2009; Smith et al. 2014; Elman et al. 2016). First, all group-level ICN spatial maps derived from all the participants (59 participants) were entered as regressors in a linear regression against each subject's preprocessed 4D functional dataset (the spatial regression procedure). This step resulted in a set of subject-specific time courses for each group-level spatial map, reflecting the mean time course of each component. These time courses were then variance-normalized to test for differences in the ICN spatial extent and amplitude. Next, these time courses were entered as regressors against the same 4D functional datasets (the temporal regression procedure) to produce a set of subject-specific spatial maps corresponding to each group-level ICN. The Z value of each voxel in these spatial maps represents the degree to which the signal fluctuation of this voxel is correlated with a given group-level ICN's mean time course. By including all 20 ICNs in both stages of the dual regression, the resulting time courses and spatial maps are partial regression estimates, in which the shared variance with other components (both physiologically plausible and artifactually related) is controlled. Then 11 networks of interest (Fig. 1A) at the group level were selected by matching a "resting state network (RSN) template maps" (Shirer et al. 2012) accompanied with visually verification (Supplementary Table 1), including the auditory network (AN), primary visual network (pVN), higher visual network (hVN), basal ganglia network (BG), anterior default mode network (aDMN), pDMN (Jones et al. 2016), lateral somatomotor network (lSMN), medial somatomotor network (mSMN), salience network (SN),

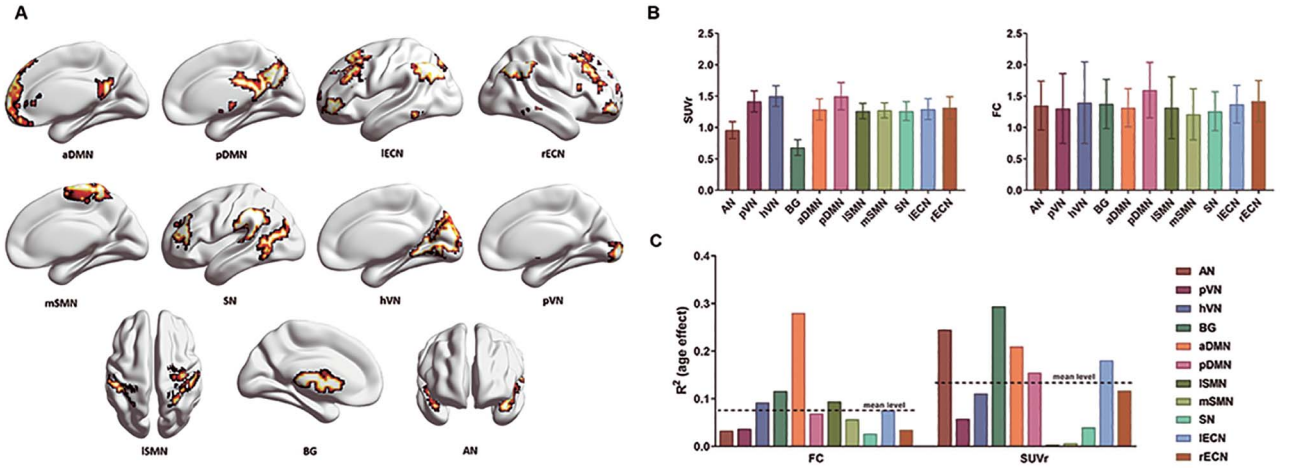

Fig. 1. Glucose metabolism and FC patterns and age-related changes of these 2 values in 11 ICNs. A) Eleven networks of interest that best matched the RSNs template maps. B) Glucose metabolism and FC patterns in each ICN. C) Age effects of FC and SUVr values in each ICN. The color bars represented the R^2 value of age effect on FC or SUVr of ICNs. Dotted lines represented the average R^2 values of FC and SUVr among all the 11 ICNs. The ICNs that both showed significant decline with age in SUVr and FC values were aDMN, BG, LECN, pDMN, and PN.

left executive control network (lECN), and right executive control network (rECN). We made 11 corresponding binarized masks based on the chosen networks with a z-score threshold at 1.0 for further analysis.

The within-subsystem FC of each 11 network in each subject was estimated by extracting the mean value from the corresponding scaled spatial maps produced from the spatial–temporal regression procedure within the corresponding binarized masks mentioned above. As previous studies have verified the spatial relationship between glucose metabolism and resting-state fMRI signal (Shah et al. 2016; Jiao et al. 2019), and to make the FDG-SUVr values and FC values comparable in the same brain region, the approach of extracting FDG-SUVr values from binarized maps derived from resting-state fMRI data was adopted. The mean FDG-SUVr values was extracted by employing ICN masks from fMRI data maps on the FDG-SUVr PET imaging maps of each subject. Finally, both the FC strength and glucose metabolism information of each ICN were acquired for each participant.

Statistical analysis

One-way analysis of variance was executed to compare the strength of glucose metabolism and FC among ICNs. The linear regression was performed to acquire the age effects of glucose metabolism and FC in each ICN. The full Pearson's correlations between the FC strength and the SUVr value in each ICN, as well as between neuroimaging characteristics and multidomain neuropsychological tests were calculated, and partial Pearson's correlations were also investigated adjusting for age, gender, and education as covariates. False Discovery Rates (FDR) multiple testing corrections were used to reduce the probability of false positives.

The mediation analyses were performed using Model 4 and Model 6 in the Hayes Process macro with SPSS (Hayes 2013) (http://www.afhayes.com/) with 5000 bootstrapped resamples. In the present study, we explored 3 kinds of mediation model. In the first model, age was the independent variable, cognitive measures that significantly correlated with age were the dependent variable, and the neuroimaging characteristics, which were correlated with both age and cognition, were the mediating variable. This analysis allowed us to determine whether the association between age and cognitive performance is mediated through the effect of age on neuroimaging characteristics (i.e. an indirect effect). In the second model, age was the independent variable, and the network FC and network SUVr were either the dependent variable or the mediating variable. This analysis allowed us to determine whether the association between age and network FC is mediated through the effect of age on network glucose metabolism or whether the association between age and glucose metabolism is mediated through the effect of age on network FC. In the third model, age was the independent variable, cognitive measure significantly correlated with age was the dependent variable, and the network FC and network SUVr were the mediating variables. Since there is no strong theoretical hypothesis to remind us which is the upstream affecting factor, we did bidirectional serial mediation analysis, and even parallel mediation analysis here to certify which mediation model is best suited to the data. These analyses were to explore more complicated relationships among age-related metabolism, the FC decline of a network, and executive function impairment. The threshold for statistical significance of path coefficients was set to $P < 0.05$.

Results

Participants' demographics and cognition characteristics

The participants' demographics and cognition characteristics of the study can be found in Table 1. They were on average 71.25 ± 7.82 years old. A total of 47% of the elders were female and the whole average education

Table 1. Demographic information and cognitive performance.

	Mean ± SD (*n* = 59)	Age effects			
		$\beta_{(age)}$	R^2	*F*	$P_{(age)}$
Age	71.25 ± 7.816	—	—	—	—
Gender(F/M)	28/31	—	—	—	—
Education	11.87 ± 4.131	—	—	—	—
General mental status					
MMSE	26.78 ± 3.222	−0.318	0.101	6.419	**0.014**
Memory function					
AVLT(N1–N5)	29.64 ± 12.204	−0.354	0.125	8.155	**0.006**
AVLT(N5)	5.48 ± 3.411	−0.341	0.116	7.513	**0.008**
ROCF-delay recall	13.80 ± 8.541	−0.299	0.090	5.604	**0.021**
Digit Span	11.61 ± 1.965	−0.102	0.010	0.603	0.441
Processing speed					
SDMT	29.55 ± 12.115	−0.324	0.105	6.669	**0.012**
TMT-A time	71.78 ± 34.59	0.247	0.061	3.688	0.060
Executive function					
TMT-B time	202.32 ± 93.375	0.302	0.091	5.740	**0.020**
Stroop C-B time	40.67 ± 26.975	0.245	0.060	3.638	0.062
Visuospatial processing					
CDT	24.72 ± 4.487	−0.206	0.042	2.518	0.118
ROCF-Copy	32.37 ± 5.657	0.000	0.000	0.000	0.999
Language ability					
CVFT	43.69 ± 13.167	−0.116	0.014	0.783	0.380
BNT	23.76 ± 3.816	−0.099	0.010	0.565	0.455

AVLT, a total score of 5 times reported; Stroop(C-B) time = Stroop Card and Word test(C-B) time.

level was 11.87 ± 4.13 years. In terms of performance on neuropsychological tests, there were significant declines in multiple cognitive domains with age, including the MMSE($R^2 = 0.101$, $P = 0.014$), AVLT (N1–N5) ($R^2 = 0.125$, $P = 0.006$), AVLT (N5) ($R^2 = 0.116$, $P = 0.008$), ROCF-delay recall($R^2 = 0.090$, $P = 0.021$), SDMT($R^2 = 0.105$, $P = 0.012$), and TMT-B time($R^2 = 0.091$, $P = 0.020$).

Strength and aging patterns of glucose metabolism and FC in each ICN

Generally, the group mean level of ^{18}F-FDG SUVr and FC strength showed a consistent pattern among ICNs: higher FC value tended to correspond with higher SUVr. For the FC aspect, the pDMN showed the highest FC level and mSMN showed the lowest level. In comparison, for the glucose metabolism aspect, the region that had the highest SUVr value was also the pDMN, well the BG showed the lowest SUVr level (Table 2; Fig. 1B). In addition, the variance of FC was larger than that of SUVr.

Among all the 11 ICNs, the ^{18}F-FDG SUVr decreases significantly with age in the AN ($r = -0.495$, df = 58, $P = 7.718E-15$), BG ($r = -0.540$, df = 58, $P = 4.663E-14$), aDMN ($r = -0.458$, df = 58, $P = 2.759E-15$), pDMN ($r = -0.394$, df = 58, $P = 0.002$), lECN ($r = -0.425$, df = 58, $P = 0.001$), rECN ($r = 0.342$, df = 58, $P = 0.008$), and hVN ($r = -0.333$, df = 58, $P = 0.010$). The aging effect of the SUVr in the aDMN($q_{(FDR)} = 3.035E-14$), AN($q_{(FDR)} = 8.49E-14$), BG($q_{(FDR)} = 5.129E-13$), lECN($q_{(FDR)} = 0.003$), pDMN($q_{(FDR)} = 0.004$), rECN ($q_{(FDR)} = 0.015$), as well as hVN ($q_{(FDR)} = 0.016$) were still significant after FDR multiple testing correction. Meanwhile, significant age effects were observed in the FC of the aDMN ($r = -0.529$, df = 58, $P = 2.364E-12$), pDMN ($r = -0.263$, df = 58, $P = 0.045$), BG ($r = -0.341$, df = 58, $P = 0.008$), hVN ($r = -0.303$, df = 58, $P = 0.020$), SMN ($r = -0.307$, df = 58, $P = 0.018$), and lECN ($r = -0.276$, df = 58, $P = 0.035$). Only the aging effects of FC in the aDMN ($q_{(FDR)} = 2.6E-11$) and BG ($q_{(FDR)} = 0.044$) were still significant after FDR correction. Taken together, the ICNs that both showed significant decline in SUVr and FC with age were the aDMN, BG, lECN, pDMN, and hVN before correction, and only the results of aDMN and BG could survive after FDR correction. (Table 2; Fig. 1C; Supplementary Fig. 2).

Correlations among aging, glucose metabolism, and FC of each ICN, and cognitive function

The Pearson's correlation coefficient between the SUVr and FC was computed in each ICN, the results showed only in the pDMN the correlation coefficient was significant ($r = 0.345$, df = 58, $P = 0.008$). By computing the partial correlation between the SUVr and FC in these ICNs after adjusting for age, gender, and education, the correlation coefficient between the SUVr and FC in the pDMN network was still significant ($r = 0.282$, df = 58, $P = 0.035$), but these results could not survive after FDR correction (Table 2; Fig. 2A).

The results of the correlation analysis showed that the SUVr value of the pDMN was significantly correlated with scores of several neuropsychological testing, including those testing general cognitive function (MMSE, $r = 0.423$, df = 58, $P = 0.001$), memory function (AVLT[N1–N5], $r = 0.391$, df = 58, $P = 0.002$; AVLT[N5], $r = 0.413$, df = 58, $P = 0.001$), processing speed (SDMT, $r = 0.323$, df = 58, $P = 0.013$; TMT-A time, $r = 0.297$, df = 58,

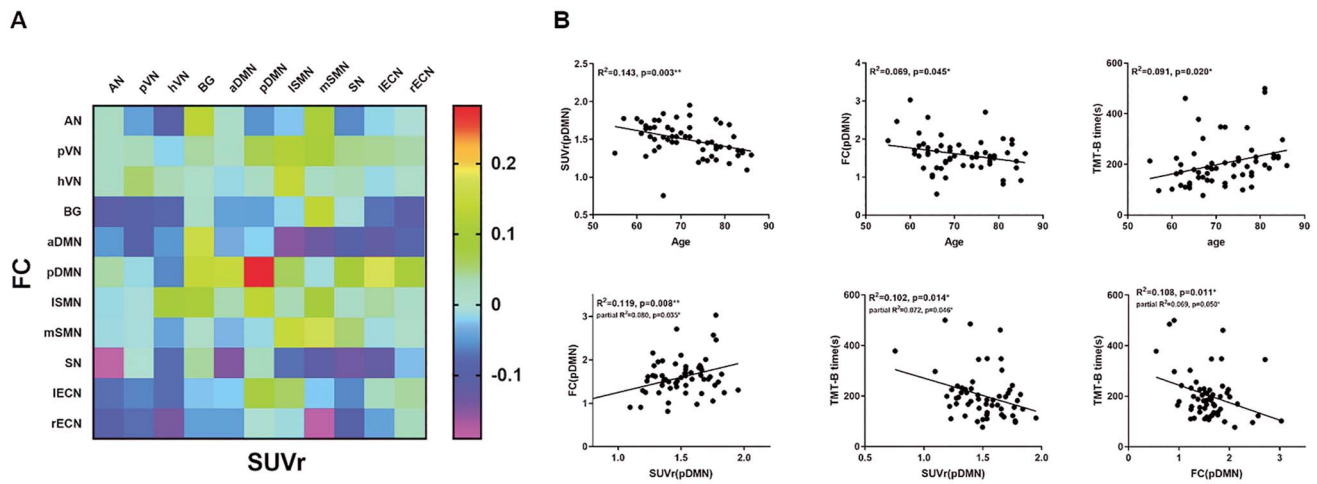

Fig. 2. Correlations among age, glucose metabolism and FC, and cognitive function. A) The partial correlation matrix between FC and SUVr combinations among ICNs. B) Some correlations among age, SUVr of pDMN, FC of pDMN, TMT-B time. Both SUVr and FC in pDMN declined significantly with age. Both SUVr and FC in pDMN were significantly correlated with TMT-B time after controlling age, gender, and education as coviariates.

$P = 0.022$), executive function (TMT-B time, $r = -0.320$, $df = 58$, $P = 0.014$), visuospatial processing (ROCF-Copy, $r = 0.295$, $df = 58$, $P = 0.024$), and language ability (CVFT, $r = 0.322$, $df = 58$, $P = 0.013$), all of these could pass the FDR correction. In comparison, the FC value of the pDMN was significantly correlated with fewer cognitive tests, mainly included tests on general cognitive function (MMSE, $r = 0.284$, $df = 58$, $P = 0.029$), processing speed (SDMT, $r = 0.281$, $df = 58$, $P = 0.031$; TMT-A time, $r = -0.283$, $df = 58$, $P = 0.030$), executive function (TMT-B time, $r = -0.328$, $df = 58$, $P = 0.011$), visuospatial processing (ROCF-Copy, $r = 0.370$, $df = 58$, $P = 0.004$), and language ability (BNT, $r = 0.384$, $df = 58$, $P = 0.003$); only TMT-B time, ROCF-Copy, and BNT could pass the FDR correction. The tests that showed significantly related to both SUVr and FC values of the pDMN were SDMT, TMT-A time, TMT-B time, and ROCF-Copy. When we calculated the partial correlation controlled with variables like age, gender, and education, the tests that showed both significantly partially related to SUVr and FC values of the pDMN left TMT-B time and ROCF-Copy. However, only the TMT-B time showed a significant difference with age ($r = -0.302$, $df = 58$, $P = 0.020$) (Table 3; Fig. 2B).

Mediation effects of glucose metabolism and FC in pDMN on executive function decline during aging

Noticing the significant correlation between aging and executive function (TMT-B time), as well as the significant correlations between executive function and the glucose metabolism and FC in the pDMN, a mediation model was built to determine whether the influence of aging on executive function decline is mediated by the pDMN's FC or its glucose metabolism. As shown in Fig. 3A, this mediation model indicated that FC of pDMN mediated the effect of aging on executive function. We did not find a similar significant mediation effect of the glucose metabolism on executive function, as the B path (mediator to outcome) was not significant ($\beta = -0.24$, $P = 0.079$, Supplementary Fig. 3A), and the bootstrap results also indicated that the mediation effect of the glucose metabolism of pDMN on executive function could not be supported by our data (indirect effect = 0.091, bootstrapped SE = 0.054, 95% confidence interval [CI] = [−0.039, 0.179]).

In another mediation model, age was set as the independent variable, FC of pDMN as the dependent variable and the glucose metabolism of pDMN as the mediating variable (Fig. 3B). This mediation model indicated that the glucose metabolism of pDMN did completely mediate the effect of age on FC of pDMN. When switching the dependent and mediating variables, such mediation effect of FC of pDMN on the association between age and the glucose metabolism of pDMN was partial (c': $\beta = 0.31$, $P = 0.015$, Supplementary Fig. 3B).

Based on the abovementioned model results, a third model was further constructed to explore the complex mediating effects of glucose metabolism and FC of pDMN on the association between age and executive function decline. The models shown in Fig. 3C and D could present a clear picture that the association between age and executive function was mediated by FC of pDMN, whereas the effect of age on FC of pDMN is further mediated by the glucose metabolism of pDMN. Finally, serial mediation analysis revealed age-related executive function deficits were mediated by glucose metabolism and FC of pDMN serially, with glucose metabolism affecting FC first. We also tested whether FC of pDMN could be a mediator at the effect of the glucose metabolism of pDMN on executive function. The results showed that this model could not be accepted because of the nonsignificant path coefficients from the SUVr(pDMN) to TMT-B time ($\beta = -0.18$, $P = 0.186$, Supplementary Fig. 3C), and the bootstrap results also confirmed that the mediation effect of the glucose metabolism of pDMN could not be supported by the

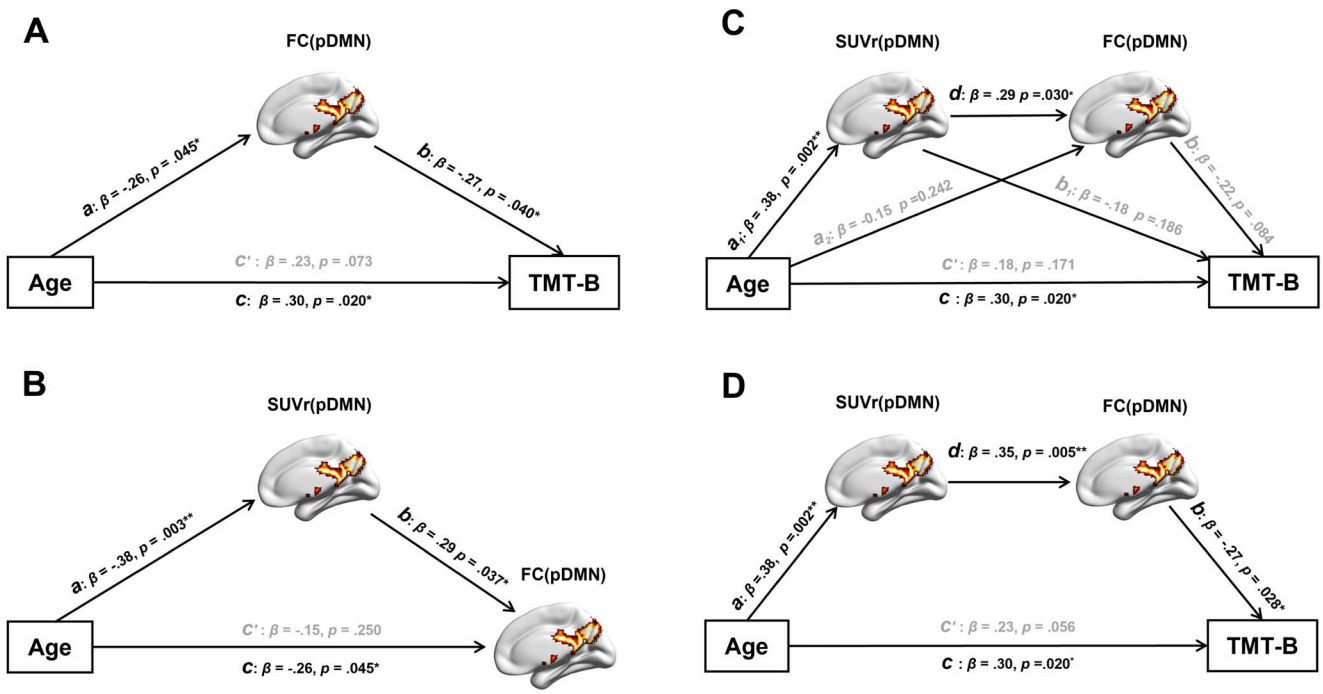

Fig. 3. The mediation analysis models. A) The model considering SUVr within pDMN as a mediating factor between age and TMT-B time. B) The model considering SUVr(pDMN) as a mediating factor between age and FC(pDMN). C) The integration serial mediation model. D) The modified serial mediation model that removed the nonsignificant paths b_1 and a_2. The path coefficients are shown beside each path. β: the standardized regression weight of each path. *: $P < 0.05$; **: $P < 0.01$; ***: $P < 0.001$.

data (indirect effect = −0.081, bootstrapped SE = 0.056, 95% CI = [−0.204, 0.007]). We finally tested the parallel mediating type model (Supplementary Fig. 3D); the results showed that this model could not be accepted neither, because the nonsignificant path coefficients from both the SUVr(pDMN) and FC(pDMN) to TMT-B time.

Discussion

Using multimodal data, the present study aimed to provide a comprehensive overview of the links between age-related metabolism decline and FC differences in some key ICNs in older adults. The results showed that the metabolic rate decreased with age predominantly in the AN, BG, hVN, aDMN, pDMN, and bilateral ECN. These metabolic differences were significantly related to cognitive performance, especially memory and executive function. Meanwhile, lower FC of the BG, hVN, aDMN, pDMN, and left ECN was also related to age. By computing the Pearson's correlation coefficient between the SUVr and FC in these 5 abovementioned ICNs that showed significant age-related decline in both brain metabolism and FC; only the SUVr and FC of pDMN showed a significant correlation coefficient between each other. Furthermore, mediation analysis suggested that age-related executive function deficits were mediated by glucose metabolism and FC of pDMN serially, with glucose metabolism affecting FC first.

During aging process, both metabolism and FC became lower in the key ICNs, including the BG, hVN, aDMN, pDMN, and lECN. Most of these ICNs belong to association regions (Huntenburg et al. 2018). Our study offers a tentative comparison of the effects of age on these 2 different neuroimaging modalities in older adults. Compared with other ICNs, metabolism in the BG network is most significantly negatively related to age, which is consistent with previous studies (Goble et al. 2012; Brown et al. 2014). The BG network plays a key role in behavior switching (Cameron et al. 2010), movement control (Hikosaka et al. 2000), and working memory regulation (Schroll and Hamker 2013). The metabolism of the DMN (aDMN and pDMN) and ECN (lECN and rECN) also showed a significant negative relationship with age (Moeller et al. 1996; Willis et al. 2002). The DMN and ECN are considered important ICNs that are vulnerable to functional deficits in aging and dementia (Leech et al. 2011).

Previous studies have documented that the DMN shows a strong correspondence between FC and metabolism (Passow et al. 2015). By using ICA analysis, multiple components, roughly at least 2 components (Damoiseaux et al. 2006; Buckner and DiNicola 2019), of the DMN could be identified. The anterior and posterior parts of the DMN have been proven to have different characteristics in lots of previous studies (Laird et al. 2011; Buckner and DiNicola 2019). In our research, FC was significantly positively related to brain metabolism only in the pDMN, suggesting that metabolism and FC of this ICN showed the most similar spatial pattern (Tahmasian et al. 2017), which is in line with the findings of previous reports (Shokri-Kojori et al. 2019). The pDMN has been suggested to be the "core node" of the DMN (Utevsky et al. 2014), which plays a very important role in brain aging.

Table 2. Age regression and correlation analysis of FC, SUVr of 18F-FDG in each ICN.

Network	FC				SUVr				Pearson correlation		Partial correlation	
	mean ± SD	$\beta_{(age)}$	R^2	F	P	mean ± SD	$\beta_{(age)}$	R^2	F	P	r	P	r	P
AN	1.35 ± 0.39	−0.182	0.033	1.96	0.167	0.92 ± 0.14	−0.495	0.245	18.47	**7.718E-15**#	0.126	0.343	0.026	0.850
pVN	1.30 ± 0.56	−0.193	0.037	2.20	0.144	1.48 ± 0.18	−0.24	0.058	3.48	0.067	0.078	0.558	0.032	0.816
hVN	1.40 ± 0.65	−0.303	0.092	5.74	**0.020**	1.53 ± 0.17	−0.333	0.111	7.090	**0.010**	0.106	0.423	0.033	0.809
BG	1.38 ± 0.39	−0.340	0.116	7.46	**0.008**#	0.64 ± 0.13	−0.542	0.294	23.72	**4.663E-14**#	0.149	0.261	0.015	0.912
aDMN	1.32 ± 0.30	−0.529	0.280	22.19	**2.364E-12**#	1.32 ± 0.30	−0.458	0.210	15.157	**2.759E-15**#	0.202	0.126	−0.037	0.787
pDMN	1.60 ± 0.44	−0.263	0.069	4.22	**0.045**	1.52 ± 0.23	−0.394	0.155	10.482	**0.002**#	**0.345**	**0.008**	**0.282**	**0.035**
lSMN	1.31 ± 0.49	−0.307	0.094	5.93	**0.018**	1.28 ± 0.12	−0.052	0.003	0.154	0.696	0.034	0.800	0.032	0.815
mSMN	1.21 ± 0.40	−0.240	0.057	3.47	0.068	1.27 ± 0.13	−0.081	0.007	0.378	0.541	0.188	0.154	0.175	0.205
SN	1.26 ± 0.31	−0.164	0.027	1.57	0.215	1.28 ± 0.16	−0.199	0.040	2.361	0.130	−0.078	0.559	−0.135	0.322
lECN	1.37 ± 0.30	−0.275	0.076	4.66	**0.035**	1.35 ± 0.18	−0.426	0.181	12.633	**0.001**#	0.095	0.475	0.027	0.841
rECN	1.42 ± 0.33	−0.188	0.035	2.10	0.153	1.35 ± 0.18	−0.342	0.117	7.572	**0.008**#	0.094	0.479	0.028	0.837

Note: Networks whose aging effect were still significant after FDR correction were marked with "#." The ICNs that both showed significant decline significantly with age in SUVr and FC values were aDMN, BG, lECN, pDMN, and hVN before correction, and only aDMN and BG survived after FDR correction. Only the correlation coefficient of FC and SUVr in pDMN was significant before correction. Partial correlation when controlling age, gender, and education did not influence this conclusion.

The pDMN, which mainly includes the PCu and the posterior cingulate gyrus (PCC) (Nelson et al. 2013; McDermott et al. 2017), seems to be particularly vulnerable to beta-amyloid (Aβ) deposition and metabolic dysfunction (Buckner et al. 2005; Fjell et al. 2014). In aging adults and those with preclinical AD (Buckner et al. 2005; Karas et al. 2007; Wolk et al. 2009), a high level of amyloid deposition induced structured and functional vulnerability in the PCu (Ikonomovic et al. 2011). Abnormal FC in the PCu was related to disrupted cognitive performance (Bai et al. 2012; Chen et al. 2017; Tao et al. 2017). The PCC has structural and functional similarities with the PCu and has also been shown to be altered in elderly subjects and AD patients (He et al. 2007).

Elaborating the relationship among brain metabolism, FC and cognition would help to improve the present understanding of the neural mechanism of cognitive decline during aging. The mediation analysis systematically described the role of metabolism in relation to age, suggesting that followed by brain metabolism disruption within the pDMN, this network was then disrupted at FC level as this highly connected functional region requires high metabolic support (Liang et al. 2013). FC appears to be critical for cognitive function (Wang et al. 2010), especially executive function (Stumme et al. 2020). The neurochemical mechanisms behind this may be related to noradrenaline, acetylcholine, and dopamine. These chemicals may modulate the connectivity of functional networks to induce cognitive decline (Shine and Poldrack 2018; Shine et al. 2019). There is a significant relationship between connectivity and neurotransmitters (Cassady et al. 2019; Lalwani et al. 2019). The preserved neurotransmitter signaling mechanisms are very important for the prevention of age-related ICN disconnections and cognitive decline.

Less metabolism appears in older adults and in patients with cognitive impairment (Coutinho et al. 2015; Arnemann et al. 2018) and may be very susceptible to age (Knopman Jr et al. 2014). Previous studies have documented a strong correspondence between FC and glucose metabolism (Tomasi et al. 2013) in DMN (Riedl et al. 2014). Our study has shown that glucose metabolism mediates age-related FC differences. It has been hypothesized that ICNs are optimized for energetically efficient communication; that is, abnormal FC may be associated with unnecessarily high amounts of energy consumption (Wig 2017). The results of mediation models could explain how metabolism reductions influence FC dysfunction and cognitive impairment during aging. However, we should be clearly aware of the shortcomings of this research; mediation analysis is still essentially a correlation analysis, and cross-sectional data prevent us from drawing any conclusions on causal effects.

In summary, we demonstrated age-related changes of FC and metabolism in the key ICNs of older adults, especially in the pDMN. More importantly, metabolism mediates the impact of FC on executive function during aging. This mediation effect suggests that metabolic

Table 3. Correlations between cognitive performance with FC and SUVr of pDMN.

Neuropsychological tests	Correlation with FC		Partial correlation with FC		Correlation with SUVr		Partial correlation with SUVr	
	r	*P*	*r*	*P*	*r*	*P*	*r*	*P*
MMSE	**0.284**	**0.029**	0.254	0.059	**0.423**	**0.001**[a]	**0.379**	**0.004**[a]
AVLT(N1–N5)	0.161	0.225	0.108	0.429	**0.391**	**0.002**[a]	**0.292**	**0.029**
AVLT(N5)	0.200	0.128	0.152	0.263	**0.413**	**0.001**[a]	**0.323**	**0.015**
ROCF-delay recall	0.227	0.084	0.151	0.266	0.231	0.078	0.140	0.302
Digit Span	0.014	0.918	0.025	0.854	0.032	0.812	0.023	0.865
SDMT	**0.281**	**0.031**	0.252	0.255	**0.323**	**0.013**[a]	0.255	0.058
TMT-A time	**−0.283**	**0.030**	-0.225	0.096	**−0.297**	**0.022**[a]	−0.252	0.061
TMT-B time	**−0.328**	**0.011**[a]	**−0.263**	**0.049**	**−0.320**	**0.014**[a]	**−0.268**	**0.046**
Stroop C-B time	0.149	0.260	0.221	0.101	−0.061	0.649	0.051	0.706
CDT	−0.003	0.984	−0.066	0.631	0.077	0.563	0.003	0.984
ROCF-Copy	**0.372**	**0.004**[a]	**0.420**	**0.001**[a]	**0.295**	**0.024**[a]	**0.343**	**0.010**
CVFT	0.192	0.145	0.167	0.219	0.322	**0.013**[a]	0.333	**0.012**
BNT	**0.384**	**0.003**[a]	**0.375**	**0.005**[a]	0.152	0.252	0.201	0.137

Note: Partial correlations of FC and SUVr of pDMN with neuropsychological tests were controlled with variables like age, gender, and education. [a]Still significant after FDR correction.

alterations in the pDMN may be especially important for understanding age-related cognitive decline. The findings may provide valuable support for future studies exploring causality between age-related metabolism and FC changes. The findings showing alterations in metabolism and FC that differ significantly throughout aging may motivate the exploration of these effects in further investigations of biomarkers and mechanisms important in brain aging.

Supplementary material

Supplementary material is available at *Cerebral Cortex* online.

Funding

This work was supported by Science and Technology Innovation 2030 Major Projects (2022ZD0211600), State Key Program of National Natural Science of China (grant number 82130118), Funds for International Cooperation and Exchange of the National Natural Science Foundation of China (grant number 81820108034), the Natural Science Foundation of China (grant number 32171085 and 31971038), and CAMS Innovation Fund for Medical Sciences (CIFMS #2021-I2M-1-025).

Conflict of interest statement: The authors thank all the volunteers and patients for their participation in the study and anonymous reviewers for their insightful comments and suggestions. There are no conflicts of interest including any financial, personal, or other relationships with people or organizations for any of the authors related to the work described in the article.

References

American Psychiatric Association. *Diagnostic and Statistical Manual of Mental Disorders (DSM-IV-TR)*. Washington, DC: American Psychiatric Association Publishing; 2000

Arenaza-Urquijo EM, Landeau B, La Joie R, Mevel K, Mezenge F, Perrotin A, Desgranges B, Bartres-Faz D, Eustache F, Chetelat G. Relationships between years of education and gray matter volume, metabolism and functional connectivity in healthy elders. *NeuroImage*. 2013:83:450–457.

Arnemann KL, Stober F, Narayan S, Rabinovici GD, Jagust WJ. Metabolic brain networks in aging and preclinical Alzheimer's disease. *NeuroImage Clin*. 2018:17:987–999.

Bai F, Shu N, Yuan Y, Shi Y, Yu H, Wu D, Wang J, Xia M, He Y, Zhang Z. Topologically convergent and divergent structural connectivity patterns between patients with remitted geriatric depression and amnestic mild cognitive impairment. *J Neurosci*. 2012:32(12):4307–4318.

Barthel H, Bullich S, Sabri O, Seibyl J, Villemagne V, Rowe C, Koglin N, Stephens A, Catafau A. F-18-Florbetaben (FBB) PET SUVR quantification: which reference region? *J Nucl Med*. 2015:56(Suppl 3):1563.

Bartzokis G. Age-related myelin breakdown: a developmental model of cognitive decline and Alzheimer's disease. *Neurobiol Aging*. 2004:25(1):5–18 author reply 49-62.

Brown RK, Bohnen NI, Wong KK, Minoshima S, Frey KA. Brain PET in suspected dementia: patterns of altered FDG metabolism. *Radiographics*. 2014:34(3):684–701.

Buckner RL, DiNicola LM. The brain's default network: updated anatomy, physiology and evolving insights. *Nat Rev Neurosci*. 2019:20(10):593–608.

Buckner RL, Krienen FM. The evolution of distributed association networks in the human brain. *Trends Cogn Sci*. 2013:17(12):648–665.

Buckner RL, Snyder AZ, Shannon BJ, LaRossa G, Sachs R, Fotenos AF, Sheline YI, Klunk WE, Mathis CA, Morris JC, et al. Molecular, structural, and functional characterization of Alzheimer's disease: evidence for a relationship between default activity, amyloid, and memory. *J Neurosci*. 2005:25(34):7709–7717.

Calhoun VD, Adali T, Pearlson GD, Pekar JJ. A method for making group inferences from functional MRI data using independent component analysis. *Hum Brain Mapp*. 2001:14(3):140–151.

Cameron IG, Watanabe M, Pari G, Munoz DP. Executive impairment in Parkinson's disease: response automaticity and task switching. *Neuropsychologia*. 2010:48(7):1948–1957.

Cassady K, Gagnon H, Lalwani P, Simmonite M, Foerster B, Park D, Peltier SJ, Petrou M, Taylor SF, Weissman DH, et al. Sensorimotor

network segregation declines with age and is linked to GABA and to sensorimotor performance. *NeuroImage*. 2019:186:234–244.

Chao Gan Y, Yu Feng Z. DPARSF: a MATLAB toolbox for "pipeline" data analysis of resting-state fMRI. *Front Syst Neurosci*. 2010:4:13.

Chen K, Reiman EM, Huan Z, Caselli RJ, Bandy D, Ayutyanont N, Alexander GE. Linking functional and structural brain images with multivariate network analyses: a novel application of the partial least square method. *NeuroImage*. 2009:47(2):602–610.

Chen Y, Liu Z, Zhang J, Chen K, Yao L, Li X, Gong G, Wang J, Zhang Z. Precuneus degeneration in nondemented elderly individuals withAPOEε4: evidence from structural and functional MRI analyses. *Hum Brain Mapp*. 2017:38(1):271–282.

Chetelat G, Landeau B, Salmon E, Yakushev I, Bahri MA, Mezenge F, Perrotin A, Bastin C, Manrique A, Scheurich A, et al. Relationships between brain metabolism decrease in normal aging and changes in structural and functional connectivity. *NeuroImage*. 2013:76:167–177.

Coutinho AM, Porto FH, Duran FL, Prando S, Ono CR, Feitosa EA, Spíndola L, de Oliveira MO, do Vale PHF, Gomes HR, et al. Brain metabolism and cerebrospinal fluid biomarkers profile of non-amnestic mild cognitive impairment in comparison to amnestic mild cognitive impairment and normal older subjects. *Alzheimers Res Ther*. 2015:7(1):58.

Damoiseaux JS, Rombouts SA, Barkhof F, Scheltens P, Stam CJ, Smith SM, Beckmann CF. Consistent resting-state networks across healthy subjects. *Proc Natl Acad Sci U S A*. 2006:103(37): 13848–13853.

Damoiseaux JS, Beckmann CF, Arigita EJS, Barkhof F, Scheltens P, Stam CJ, Smith SM, Rombouts SARB. Reduced resting-state brain activity in the "default network" in normal aging. *Cereb Cortex*. 2008:18(8):1856–1864.

Douaud G, Groves AR, Tamnes CK, Westlye LT, Duff EP, Engvig A, Walhovd KB, James A, Gass A, Monsch AU, et al. A common brain network links development, aging, and vulnerability to disease. *Proc Natl Acad Sci U S A*. 2014:111(49):17648–17653.

Elman JA, Madison CM, Baker SL, Vogel JW, Marks SM, Crowley S, O'Neil JP, Jagust WJ. Effects of beta-amyloid on resting state functional connectivity within and between networks reflect known patterns of regional vulnerability. *Cereb Cortex*. 2016:26(2): 695–707.

Ferreira LK, Busatto GF. Resting-state functional connectivity in normal brain aging. *Neurosci Biobehav Rev*. 2013:37(3):384–400.

Filippini N, MacIntosh BJ, Hough MG, Goodwin GM, Frisoni GB, Smith SM, Matthews PM, Beckmann CF, Mackay CE. Distinct patterns of brain activity in young carriers of the APOE-epsilon4 allele. *Proc Natl Acad Sci U S A*. 2009:106(17):7209–7214.

Fjell AM, Mcevoy L, Holland D, Dale AM, Walhovd KB. What is normal in normal aging? Effects of aging, amyloid and Alzheimer's disease on the cerebral cortex and the hippocampus. *Prog Neurobiol*. 2014:117:20–40.

Goble DJ, Coxon JP, Van Impe A, Geurts M, Van Hecke W, Sunaert S, Wenderoth N, Swinnen SP. The neural basis of central proprioceptive processing in older versus younger adults: an important sensory role for right putamen. *Hum Brain Mapp*. 2012:33(4): 895–908.

Good CD, Johnsrude I, Ashburner J, Henson RNA, Friston KJ, Frackowiak RSJ. Cerebral asymmetry and the effects of sex and handedness on brain structure: a voxel-based morphometric analysis of 465 normal adult human brains. *NeuroImage*. 2001:14(1): 21–36.

Greicius MD, Srivastava G, Reiss AL, Menon V. Default-mode network activity distinguishes Alzheimer's disease from healthy aging: evidence from functional MRI. *Proc Natl Acad Sci U S A*. 2004:101(13):4637–4642.

Gusnard DA, Raichle ME, Raichle ME. Searching for a baseline: functional imaging and the resting human brain. *Nat Rev Neurosci*. 2001:2:685–694.

Hayes AF. *Introduction to mediation, moderation, and conditional process analysis: a regression-based approach*. New York (NY): The Guilford Press; 2013

He Y, Wang L, Zang Y, Tian L, Zhang X, Li K, Jiang T. Regional coherence changes in the early stages of Alzheimer's disease: a combined structural and resting-state functional MRI study. *NeuroImage*. 2007:35(2):488–500.

Hikosaka O, Takikawa Y, Kawagoe R. Role of the basal ganglia in the control of purposive saccadic eye movements. *Physiol Rev*. 2000:80(3):953–978.

Hsieh TC, Lin WY, Ding HJ, Sun SS, Wu YC, Yen KY, Kao CH. Sex- and age-related differences in brain FDG metabolism of healthy adults: an SPM analysis. *J Neuroimaging*. 2012:22(1):21–27.

Huntenburg JM, Bazin PL, Margulies DS. Large-scale gradients in human cortical organization. *Trends Cogn Sci*. 2018:22(1):21–31.

Ikonomovic M, Klunk W, Abrahamson E, Wuu J, Mathis C, Scheff S, Mufson E, DeKosky S. Precuneus amyloid burden is associated with reduced cholinergic activity in Alzheimer disease. *Neurology*. 2011:77(1):39–47.

Jiao F, Gao Z, Shi K, Jia X, Wu P, Jiang C, Ge J, Su H, Guan Y, Shi S, et al. Frequency-dependent relationship between resting-state fMRI and glucose metabolism in the elderly. *Front Neurol*. 2019:10:566.

Jones DT, Knopman DS, Gunter JL, Graff-Radford J, Vemuri P, Boeve BF, Petersen RC, Weiner MW, Jack CR Jr, Alzheimer's Disease Neuroimaging I. Cascading network failure across the Alzheimer's disease spectrum. *Brain*. 2016:139(2):547–562.

Kalpouzos G, Chetelat G, Baron JC, Landeau B, Mevel K, Godeau C, Barre L, Constans JM, Viader F, Eustache F, et al. Voxel-based mapping of brain gray matter volume and glucose metabolism profiles in normal aging. *Neurobiol Aging*. 2009:30(1): 112–124.

Karas G, Scheltens P, Rombouts S, van Schijndel R, Klein M, Jones B, van der Flier W, Vrenken H, Barkhof F. Precuneus atrophy in early-onset Alzheimer's disease: a morphometric structural MRI study. *Neuroradiology*. 2007:49(12):967–976.

Knopman DS Jr, Jack CR Jr, Wiste HJ, Lundt ES, Weigand SD, Vemuri P, Lowe VJ, Kantarci K, Gunter JL, Senjem ML, et al. 18F-fluorodeoxyglucose positron emission tomography, aging, and apolipoprotein E genotype in cognitively normal persons. *Neurobiol Aging*. 2014:35(9):2096–2106.

Laird AR, Fox PM, Eickhoff SB, Turner JA, Ray KL, McKay DR, Glahn DC, Beckmann CF, Smith SM, Fox PT. Behavioral interpretations of intrinsic connectivity networks. *J Cogn Neurosci*. 2011:23(12): 4022–4037.

Lalwani P, Gagnon H, Cassady K, Simmonite M, Peltier S, Seidler RD, Taylor SF, Weissman DH, Polk TA. Neural distinctiveness declines with age in auditory cortex and is associated with auditory GABA levels. *NeuroImage*. 2019:201:116033.

Leech R, Kamourieh S, Beckmann CF, Sharp DJ. Fractionating the default mode network: distinct contributions of the ventral and dorsal posterior cingulate cortex to cognitive control. *J Neurosci*. 2011:31(9):3217–3224.

Liang X, Zou Q, He Y, Yang Y. Coupling of functional connectivity and regional cerebral blood flow reveals a physiological basis for network hubs of the human brain. *Proc Natl Acad Sci U S A*. 2013:110(5):1929–1934.

Lu H, Zhang J, Liang Y, Qiao Y, Yang C, He X, Wang W, Zhao S, Wei D, Li H, et al. Network topology and machine learning analyses reveal microstructural white matter changes underlying Chinese medicine Dengzhan Shengmai treatment on patients with vascular cognitive impairment. *Pharmacol Res*. 2020:156: 104773.

Manza P, Wiers CE, Shokri-Kojori E, Kroll D, Feldman D, Schwandt M, Wang GJ, Tomasi D, Volkow ND. Brain network segregation and glucose energy utilization: relevance for age-related differences in cognitive function. *Cereb Cortex*. 2020:30(11):5930–5942.

McDermott KB, Gilmore AW, Nelson SM, Watson JM, Ojemann JG. The parietal memory network activates similarly for true and associative false recognition elicited via the DRM procedure. *Cortex*. 2017:87:96–107.

Moeller JR, Ishikawa T, Dhawan V, Spetsieris P, Mandel F, Alexander GE, Grady C, Pietrini P, Eidelberg D. The metabolic topography of normal aging. *J Cereb Blood Flow Metab*. 1996:16(3):385–398.

Mosconi L. Brain glucose metabolism in the early and specific diagnosis of Alzheimer's disease. *Eur J Nucl Med Mol Imaging*. 2005:32(4):486–510.

Nelson SM, Arnold KM, Gilmore AW, McDermott KB. Neural signatures of test-potentiated learning in parietal cortex. *J Neurosci*. 2013:33(29):11754–11762.

Passow S, Specht K, Adamsen TC, Biermann M, Brekke NL, Craven AR, Ersland L, Grüner R, Kleven-Madsen N, Kvernenes OH, et al. Default-mode network functional connectivity is closely related to metabolic activity. *Hum Brain Mapp*. 2015:36(6):2027–2038.

Riedl V, Bienkowska K, Strobel C, Tahmasian M, Grimmer T, Forster S, Friston KJ, Sorg C, Drzezga A. Local activity determines functional connectivity in the resting human brain: a simultaneous FDG-PET/fMRI study. *J Neurosci*. 2014:34(18):6260–6266.

Schroll H, Hamker FH. Computational models of basal-ganglia pathway functions: focus on functional neuroanatomy. *Front Syst Neurosci*. 2013:7:122.

Shah D, Deleye S, Verhoye M, Staelens S, Van der Linden A. Resting-state functional MRI and [18F]-FDG PET demonstrate differences in neuronal activity between commonly used mouse strains. *NeuroImage*. 2016:125:571–577.

Shine JM, Poldrack RA. Principles of dynamic network reconfiguration across diverse brain states. *NeuroImage*. 2018:180(Pt B): 396–405.

Shine JM, Breakspear M, Bell PT, Ehgoetz Martens KA, Shine R, Koyejo O, Sporns O, Poldrack RA. Human cognition involves the dynamic integration of neural activity and neuromodulatory systems. *Nat Neurosci*. 2019:22(2):289–296.

Shirer WR, Ryali S, Rykhlevskaia E, Menon V, Greicius MD. Decoding subject-driven cognitive states with whole-brain connectivity patterns. *Cereb Cortex*. 2012:22(1):158–165.

Shokri-Kojori E, Tomasi D, Alipanahi B, Wiers CE, Wang GJ, Volkow ND. Correspondence between cerebral glucose metabolism and BOLD reveals relative power and cost in human brain. *Nat Commun*. 2019:10(1):690.

Smith DV, Utevsky AV, Bland AR, Clement N, Clithero JA, Harsch AE, McKell Carter R, Huettel SA. Characterizing individual differences in functional connectivity using dual-regression and seed-based approaches. *NeuroImage*. 2014:95:1–12.

Stumme J, Jockwitz C, Hoffstaedter F, Amunts K, Caspers S. Functional network reorganization in older adults: graph-theoretical analyses of age, cognition and sex. *NeuroImage*. 2020:214:116756.

Tahmasian M, Drzezga A, Savio A, Rachakonda S, Sorg C. Resting-state networks as simultaneously measured with functional MRI and PET. *J Nucl Med*. 2017:58(8):1314–1317.

Tao W, Li X, Zhang Z. Increased functional connectivity of default mode network in patients with moderate amnestic mild cognitive impairment: inflection point in course of disease. *Alzheimers Dement*. 2017:13(7S_Part_9):P460.

Tomasi D, Wang GJ, Volkow ND. Energetic cost of brain functional connectivity. *Proc Natl Acad Sci U S A*. 2013:110(33):13642–13647.

Utevsky AV, Smith DV, Huettel SA. Precuneus is a functional Core of the default-mode network. *J Neurosci*. 2014:34(3):932–940.

van den Heuvel MP, Sporns O, Collin G, Scheewe T, Mandl RCW, Cahn W, Goñi J, Hulshoff Pol HE, Kahn RS. Abnormal rich club organization and functional brain dynamics in schizophrenia. *JAMA Psychiat*. 2013:70(8):783–792.

Verger A, Roman S, Chaudat RM, Felician O, Ceccaldi M, Didic M, Guedj E. Changes of metabolism and functional connectivity in late-onset deafness: evidence from cerebral (18)F-FDG-PET. *Hear Res*. 2017:353:8–16.

Wagner G, Gussew A, Kohler S, de la Cruz F, Smesny S, Reichenbach JR, Bar KJ. Resting state functional connectivity of the hippocampus along the anterior-posterior axis and its association with glutamatergic metabolism. *Cortex*. 2016:81:104–117.

Wang L, Liu X, Guise KG, Knight RT, Ghajar J, Fan J. Effective connectivity of the fronto-parietal network during attentional control. *J Cogn Neurosci*. 2010:22(3):543–553.

Wang L, Li H, Liang Y, Zhang J, Li X, Shu N, Wang YY, Zhang Z. Amnestic mild cognitive impairment: topological reorganization of the default-mode network. *Radiology*. 2013:268(2):501–514.

Wig GS. Segregated systems of human brain networks. *Trends Cogn Sci*. 2017:21(12):981–996.

Willis MW, Ketter TA, Kimbrell TA, George MS, Herscovitch P, Danielson AL, Benson BE, Post RM. Age, sex and laterality effects on cerebral glucose metabolism in healthy adults. *Psychiatry Res*. 2002:114(1):23–37.

Wolk DA, Price JC, Saxton JA, Snitz BE, James JA, Lopez OL, Aizenstein HJ, Cohen AD, Weissfeld LA, Mathis CA, et al. Amyloid imaging in mild cognitive impairment subtypes. *Ann Neurol*. 2009:65(5): 557–568.

Yang C, Li X, Zhang J, Chen Y, Li H, Wei D, Lu P, Liang Y, Liu Z, Shu N, et al. Early prevention of cognitive impairment in the community population: the Beijing Aging Brain Rejuvenation Initiative. *Alzheimers Dement*. 2021:17(10):1610–1618.

Yuan J, Guan H, Zhou X, Niu N, Li F, Cui L, Cui R. Changing brain metabolism patterns in patients with ANMDARE: serial 18F-FDG PET/CT findings. *Clin Nucl Med*. 2016:41(5):366–370.

Zhang HY, Chen WX, Jiao Y, Xu Y, Zhang XR, Wu JT. Selective vulnerability related to aging in large-scale resting brain networks. *PLoS One*. 2014:9(10):e108807.